A low-cost tonometer alternative: a comparison between photoplethysmogram and finger ballistocardiogram and validation against tonometric waveform.

JANJUA, G.M.W., FINLAY, D., GULDENRING, D., HAQ, A.U. and MCLAUGHLIN, J.

2019

Received August 2, 2019, accepted September 19, 2019, date of publication September 27, 2019,
date of current version October 11, 2019.

Digital Object Identifier 10.1109/ACCESS.2019.2944212

A Low-Cost Tonometer Alternative: A Comparison Between Photoplethysmogram and Finger Ballistocardiogram and Validation Against Tonometric Waveform

GHALIB MUHAMMAD WAQAS JANJUA, (Member, IEEE), DEWAR FINLAY, (Member, IEEE), DANIEL GULDENRING, ATTA UL HAQ, AND JAMES MCLAUGHLIN, (Member, IEEE)
Nibec Nanotechnology and Bioengineering Centre (NIBEC), Ulster University, Belfast BT37 0QB, U.K.

Corresponding author: Ghalib Muhammad Waqas Janjua (g.janjua@ ulster.ac.uk)

This work was supported by the European Union's Horizon 2020 Research and Innovation Program through the Marie Sklodowska-Curie Grant under Agreement 676201.

ABSTRACT Hypertension is a silent killer and one-third of its sufferers are unaware of its presence. Tonometric devices, like SphygmoCor, Compilor etc., represent the gold standard in pulse wave velocity (PWV) and augmentation index (AIx) measurements which are limited by their high cost and operational accuracy. Here, we present an alternative technology that is low cost and may be suitable for the 'wearable' setting. We undertook the comparisons of arterial waveforms obtained by photoplethysmogram (PPG) and finger ballistocardiogram (BPP) sensors which were then validated against a SphygmoCor tonometric device. Specifically, the agreement analysis of the augmentation, stiffness, reflection, elasticity, ejection elasticity and dicrotic reflection indexes showed that arterial distension waveform sensing using BPP sensor, has precision and accuracy similar to that of a SphygmoCor tonometric device whilst outperforming the volumetric arterial flow sensing using a PPG sensor, in every index. BPP indexes showed the r^2 fit of up to 0.95 and Spearman's rank correlation up to 0.91 when validated against the SphygmoCor tonometer. The estimated individual transfer functions for the BPP sensor, with reference to SphygmoCor, have accuracies of above 85% and 98% for 2 and 4-element windkessel (WK) models, respectively. The findings reported in this work may also be useful for the development of systems that are beneficial in the early and/or routine detection of hypertension.

INDEX TERMS Augmentation index (AIx), finger ballistocardiogram (BPP), cuff-less blood pressure, electrocardiogram (ECG), photoplethysmogram (PPG), pulse wave velocity (PWV), stiffness index (SI), reflection index (RI).

I. INTRODUCTION

Hypertension is a silent killer and reported to be prevalent in 1.13 billion adults worldwide in 2015. Arterial stiffness [1], [2] is one of the leading causes of hypertension and cardiovascular diseases. Aortic stiffness increases the burden on the left ventricle and consistent and/or longer duration of the condition results in lower ejection fraction. Eventually, this results in wear and tear to the heart muscles and increases the chances of heart failure, seizures, and strokes events. It causes chronic cardiovascular diseases which in turn significantly increases the cost of healthcare. Earlier detection can control the cardiovascular morbidity & mortality and their forerun interventions can cure the issue through minor changes to daily lifestyle that do not require further medical intervention – even in the form of prescribed medications [3].

Many new technologies [1], [4] have been developed and old technologies augmented in order to provide bio-signal monitoring and the associated analyses of arterial waveforms, in a wearable device for the assessment of augmentation indexes [5], [6]. However, the detection of hypertension through the monitoring of blood pressure has not seen the advances that other areas such ECG and heart rate monitoring because the technology that allows easy non-obtrusive reliable blood pressure monitoring has yet to be realized.

The aim of the presented work is to investigate novel unobtrusive/modest methods for the assessment of arterial stiffness which could, in turn, be used to predict

The associate editor coordinating the review of this manuscript and approving it for publication was Michele Magno.

cardiovascular risk. This study collates a novel dataset which compares arterial stiffness indexes on BPP and PPG arterial waveforms and validates against the SphygmoCor tonometric arterial waveform. This novel dataset compares and validates the arterial waveforms at the distal phalanx to radial arterial waveform. Their agreement analysis examines the functional parameters* such as stiffness index (SI), reflection index (RI), aging index (AI), augmentation index (AIx), elasticity index (EI), cardiac ejection elasticity index (EEI) and dicrotic reflection index (Dai). The results are reproducible with an accuracy comparable to the maned operated SphygmoCor tonometer device.

II. BACKGROUND

In 1877 J. W. Gordon first illustrated the concept of the ballistocardiogram (BCG) in this paper where he showed the movement of the needle, due to blood ejected from the heart, whilst standing on a weight scale [8]. In more recent years, there has been a renewed interest in the BCG with more recent studies illustrating the effect of embedding BCG technology in pervasive items such as chairs, beds, weight scale and body worn items [7].

In 1903 the Noble Laureate Willem Einthoven invented the ECG which measures the electrical activity of the heart and the most commonly practiced test in diagnosing heart related diseases.

In 1938 Hertzman discovered the relationship between backscattered light and volumetric blood flow, the phenomenon known as photoplethysmography [8]. It non-invasively measures the oxygenation saturation level which are used in primary health care systems daily.

In 1862 Von Graefe made the indentation tonometer to measure the pressure of the eyeball and in 1867 his pupil Weber made the applanation tonometer [9]. Goldmann applanation tonometry principle states that when an artery is flattened against the bone by a force, until its diameter becomes zero, then the internal pressure is equal to the externally applied pressure [10].

This study focuses on the assessment of the arterial stiffness to keep the track of vital signs in a wearable setting through a subject normal day routine. The blood pressure (BP) is a key parameter to diagnose hypertension and arterial stiffness is a pre-cursor to this stage. This study is part of our continuing research [11] and future works are planned to test hypertensive subjects in a clinical environment.

III. MATHEMATICAL BACKGROUND

The heart pumps the blood in a non-continuous way to the aorta, which works under WK principle (electrical analogy of RC parallel circuit shown in figure 1 and described in equations (1&2) and forms the continuous flow.

$$P(t) = I(t)^{*}r + P_c(t) \tag{1}$$

$$I(t) = \frac{P_c(t)}{R} - C\frac{dP_c(t)}{dt} \tag{2}$$

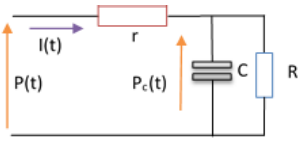

FIGURE 1. An electrical analogy of 3-element Windkessel model of an arterial branch.

where arterial flow analogous to electrical model parameters are: '$P(t)$' is an aorta blood pressure in mmHg, '$I(t)$' is a blood flow from heart in cm^3/s, 'r' is an aortic blood flow resistance in mmHg x s/cm^3, $P_c(t)'$ is an aortic compliance in $cm^3/mmHg$, 'C' is an arterial compliance in $cm^3/mmHg$ and 'R' is a systematic arterial system peripheral resistance in mmHg x s/cm^3.

By using state space canonical representation and the Laplace transformation, it is possible to describe the transfer function of the 3-element WK model as:

$$H(s) = \frac{R}{RC_s + 1} + r \tag{3}$$

Propagation of PWV depends on the elasticity of the arteries i.e. stiffer the arteries the higher the PWV. This relationship is described in Moens-korteweg (equation 4) [12].

$$PWV = \sqrt{\frac{Eh}{\rho d}} \tag{4}$$

where, 'E' is a Young's modulus of the arterial wall; 'h' is the wall thickness; 'd' is the arterial diameter and 'ρ' is the blood density.

Pulse pressure is the pulse height of an arterial waveform which is the volumetric difference between systolic and diastolic peaks which inherit the hemodynamic characteristics. Waveform analysis can demonstrate the outcome of the hemodynamic parameter and arterial stiffness indexes.

IV. MATERIAL AND METHODS

The Biopac MP36R unit (Biopac System, USA) was used for the simultaneous acquisition of electrocardiogram (ECG), photoplethysmogram (PPG), SphygmoCor tonometer (SPH) and finger ballistocardiogram (BPP) signals. The acquisition device has four synchronized acquisition channels which digitize the data at a sample rate of 2 kHz with a resolution of 24-bits, in real-time. The acquisition device is serially connected to a PC (Windows 10 OS) through AcqKnowledge 4 software which enables data analysis and export. The system block diagram is shown in Figure 2.

We captured the ECG signal which provided the reference location of the cardiac cycles for analyzing the rest of the captured signals. Three electrodes were placed proximally (i.e. on the left shoulder, right shoulder and at the pubis) to capture Einthoven lead-1. The chest area provides the stable anchoring position for the ECG signal which limits noise and motion artefacts. Before placing the electrodes, the subject's skin was cleaned with non-alcoholic wipes and hair was removed to make a good surface contact. Biopac SS2LB lead

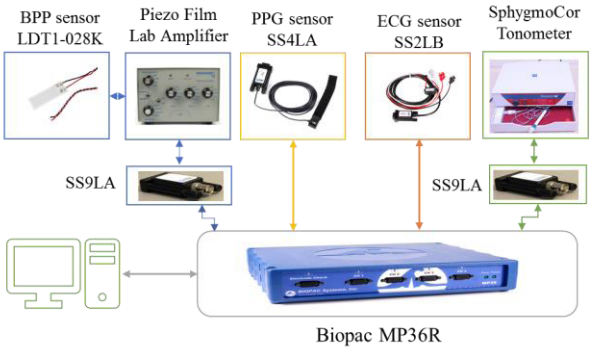

FIGURE 2. The signal acquisition system block diagram.

TABLE 1. Configuration parameters for piezo file lab amplifier.

Mode	Voltage—1G (50pF)
Filter low frequency	0.1Hz
Filter high frequency	10Hz
Gain	10dB typical
Power	9V Battery

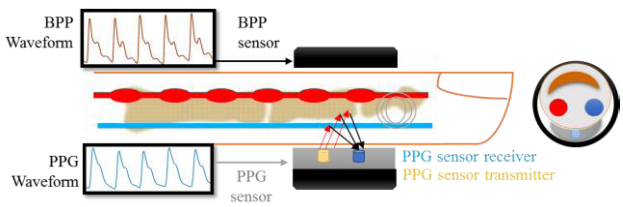

FIGURE 3. The stacking of BPP and reflective PPG sensors on index finger lateral view (on left) and cross-sectional view (on right).

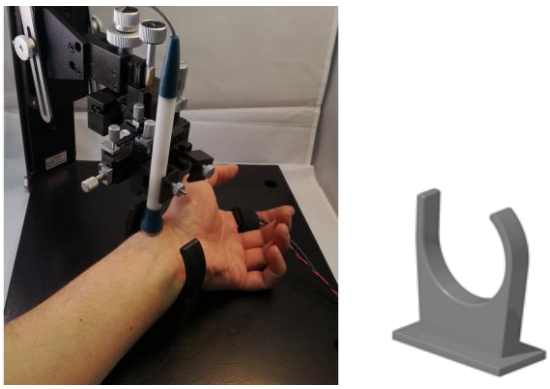

FIGURE 4. The 3D printed fixture to hold the wrist (on right) and acquisition scenario (left).

was used to capture the data on channel 1 of Biopac MP36R unit.

We placed the PPG sensor at the distal phalanx of the index finger, to capture the volumetric flow of the radialis indicis artery. A photodiode of 960 nm wavelength was used to illuminate the finger area and changes were captured at a photodetector, corresponding to the optical absorption in volumetric blood flow. The wavelength of 960 nm penetrates the greatest depth in hypodermis layer [13] which gets the response from radialis indicis artery at the distal phalanx in the index digit. The reflectance sensing technique provided enough backscattering for the experiment. The skin of a subject was cleaned with alcoholic wipes before sensor placement. Biopac SS4LA lead was used to capture the data on Channel 2 of Biopac MP36R unit.

We used a Polyvinylidene Fluoride (PVDF) piezoelectric sensor [14] to measure the distension waveform of radialis indicis artery due to pulsating blood flow (named as finger ballistocardiogram (BPP)). The PVDF piezoelectric sensor (Measurement Specialist Ltd., USA) was used and its output was interfaced to an amplifier (Piezo Film Lab amplifier by Measurement Specialist). The sensor surface was insulated with electrostatic tape to isolate it from skin contact. The sensor amplifier setting is shown in table 1. The output of an amplifier was interfaced with SS9LA lead through a BNC cable at Channel 4 of Biopac MP36R unit. The sensor was wrapped on top of the PPG sensor fixture and strapped around the distal phalanx of the index finger. The stacking of the BPP sensor over the PPG sensor gave the vertical spatial alignment for a single point simultaneous acquisition of the waveforms. The configuration of BPP and PPG sensors on the index finger is shown in Figure 3.

The SphygmoCor (AtCor Medical, Australia) tonometry system's (SPH) limited version, with the analog output of tonometer, was used for capturing applanation tonometric data at the radial artery. The output of the system was acquired with the SS9LA interface, as an analog signal, at channel 3 of the Biopac MP36R unit. We selected the radial artery for applanation across the radius bone. We used a micro-manipulator, with six degrees of freedom, for the unaided human operation to achieve a consistent minimum acceptable operator index of 85%. The micromanipulator provided the best repeatability and accuracy in the signal acquisition in our experiment. The radial artery at the wrist was propped with the help of a semi-circular fixture. We 3D printed a fixture, using a Fortus 380mc 3D printer, semi-circular wrist clamp for subjects as shown in Figure 4. The radial artery was palpated and marked to align the tip of the tonometer accurately. For each subject, tonometer vertical pressure was adjusted manually by observing the saturation/clipping in the arterial waveform in the SphygmoCor system suite.

A Huntleigh Smartsigns LitePlus Vital Signs Monitor was used to measure the brachial blood pressure of subjects with medium size arm cuff in a seated posture. The Nokia Body Cardio scale was used to measure subject's weight in kilograms. The subject's height was measured with a wall mounted height measurement scale. The Subject's mood and time since food and coffee were last ingested, was recorded before measurement. All the sensors were placed on the subject's left-hand index digits. The room temperature was controlled at 22° C.

The study compared with dimensionless units as waveforms were normalized and we have not quantized and/or quantified the sensor's waveforms with reference to blood oxygenation and pressure levels in the artery. We have

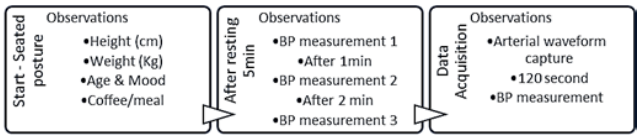

FIGURE 5. Flow chart of data collection protocol.

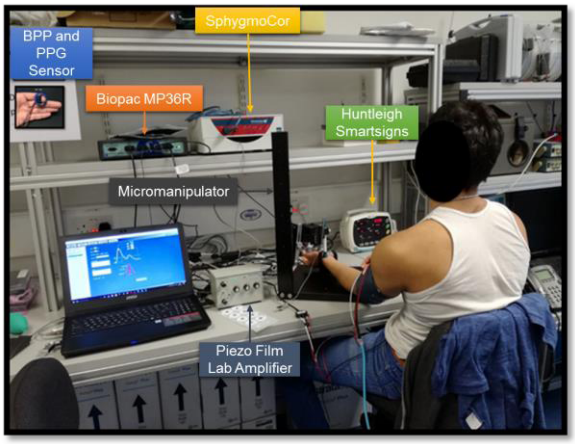

FIGURE 6. The arterial waveforms signal acquisition environment of the subject 11 – same for all of the subjects in the study.

neglected the hydrostatic and gravitation effect by keeping the same height and posture consistent across all the subjects.

We have conducted this study in 14 healthy volunteers of age 36±6 years with mixed ethnic background. For this study, ethics of experiment followed the Helsinki declaration and approval was obtained by the local research ethics committee, IRAS Project ID 166742. Subjects were asked to refrain from consuming alcohol for 36 hours before the data collection. They were also instructed not to take any food meal or coffee 2 hours before the data collection. The study protocol is shown in Figure 5 and acquisition environment is shown in Figure 6.

V. FIDUCIAL ANALYSIS

The captured arterial waveform plot of SPH, PPG and BPP signal is shown in Figure 7. The fiducial points [15] of the wave are marked in the Figure 8 and their descriptions are: 'S' represents the diastolic peak of blood pulse in the artery – it shows the aortic valve opening point and lowest pressure of blood flow; 'P' represents the systolic peak of blood flow in the artery – it shows the highest pressure point of the blood flow; 'T' represents the tidal wave of blood flow in the artery – it shows the reflected wave by smaller arteries; 'C' represents the incisura wave of blood flow in the artery – it shows the aortic valve closure; 'D' represents the dicrotic wave of blood flow in artery – it shows the reflected pressure wave.

The fiducial points [5] of the second derivative, also called accelerated plethysmography (APG), are shown in Figure 9. APG waveforms are: 'a-wave' is a pre-systolic positive peak of APG; 'b-wave' is the pre-systolic negative peak of APG; 'c-wave' is the post-systolic crest of APG: 'd-wave' posts systolic trough and 'e-wave' align with incisura wave. In healthy subjects, ratios of b-wave with respect to a-wave increase with age and vice versa for rest of the waves [15]. Information regarding arterial indexes can be found in supplementary document.

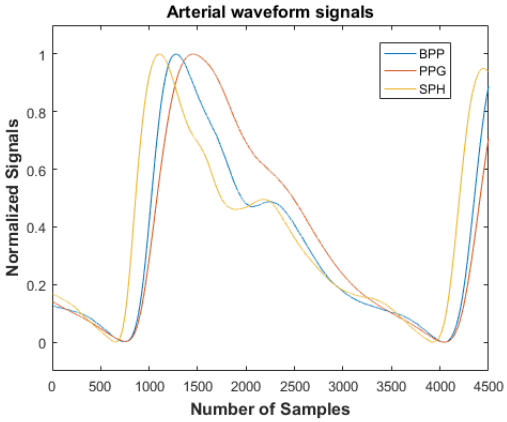

FIGURE 7. The example plots of oversample data at 4500 sample per second of 1.4 RR of SPH, PPG and BPP signals of the subject 7.

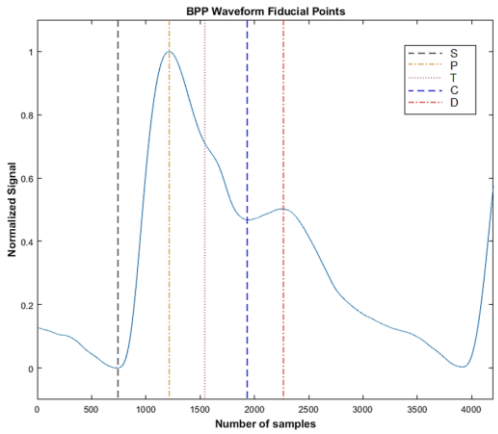

FIGURE 8. An arterial waveform where the fiducial points (S, P, T, C and D) have been highlighted with the dashed lines.

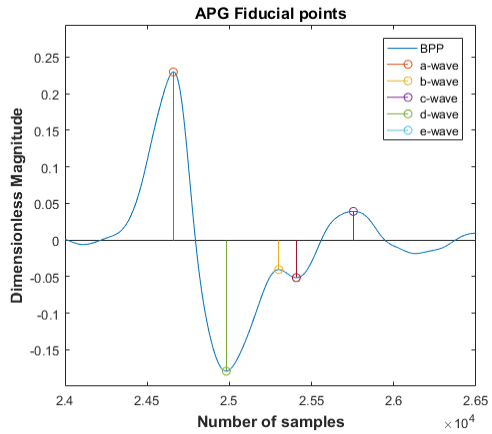

FIGURE 9. The APG waveform representing the fiducial locations (a, b, c, d, and e) as indicated in the graph.

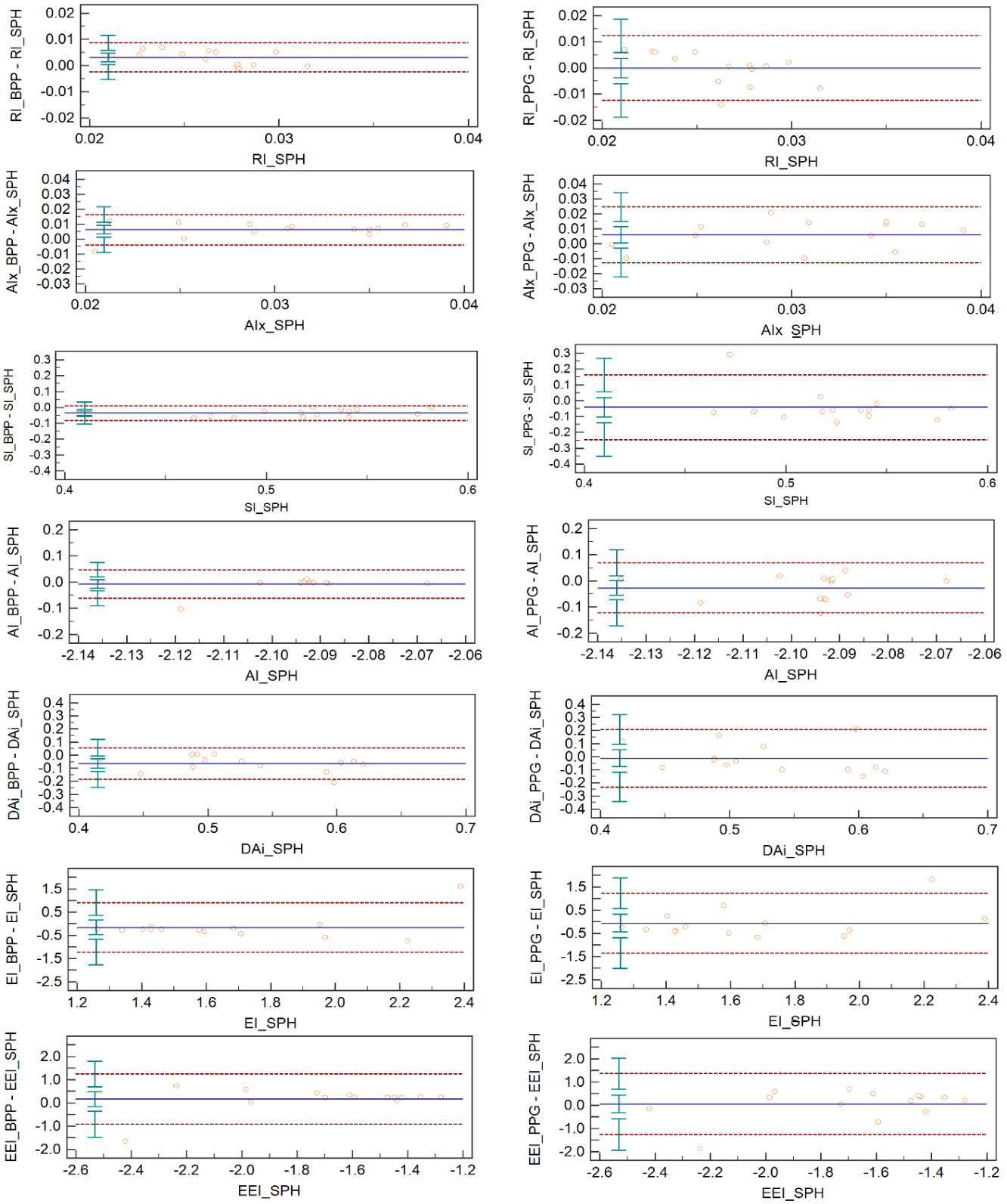

FIGURE 10. The Bland-Altman plots, SPH against BPP waveform indexes (on right) and SPH against PPG waveform indexes (on left)- dotted red line shows 1.96SD of agreement analysis.

VI. DIGITAL SIGNAL PROCESSING

The data was initially recorded/stored in raw ascii text format then data was imported into the MATLAB platform (Mathworks, USA) for signal processing. The data was manually inspected and cropped to remove signal noise due to motion artefact. The PPG, SPH and BPP signal were filtered

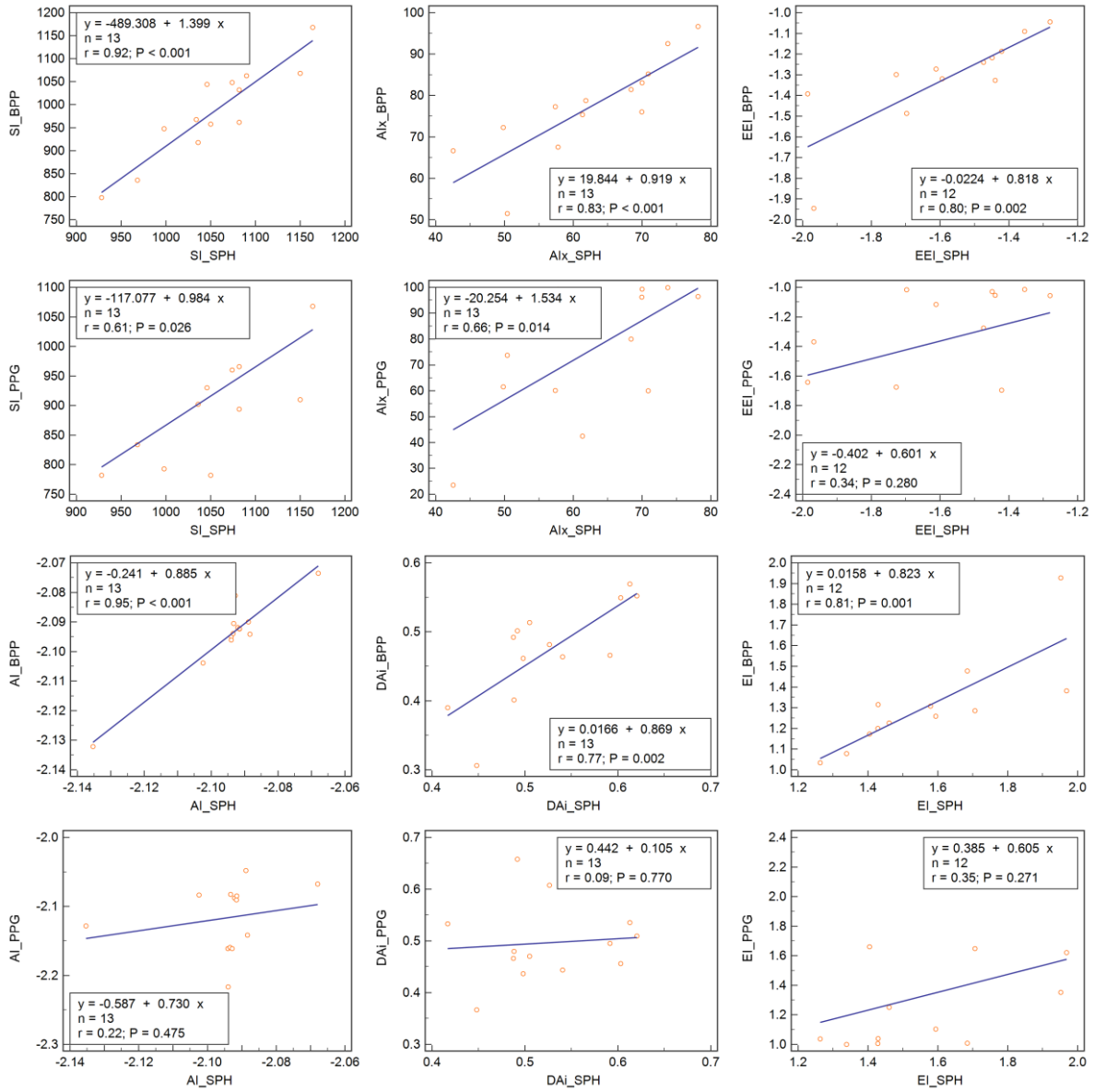

FIGURE 11. The regression analysis of arterial indexes, SPH against BPP waveform indexes (on top) and SPH against PPG waveform indexes (on bottom), respectively for each pair of rows (doesn't include RI index due to in significant correlation values).

with a least square technique using a Savitzky-Golay filter, as it is better than FIR filter in preserving higher frequency component of signal, filter with -3db at 41Hz. The Pans-Tompkins algorithm [16] was used to detect and mark the ECG R-wave and this was taken as the gating location of each cardiac cycle for rest of the arterial signals. Data SNR got increased in the arterial waveform signals by ensemble averaging for 10-second windows at R-peak of ECG for the signal which were within a standard deviation of ± 1. The following algorithm steps was implemented on steady periods of cohort data, steps are as follows:

1) Signal pre-processing and filtering
2) Detrending and normalization of the signals
3) ECG R-peak was detected
4) The ensemble average of the PPG, BPP and SPH signals were calculated at R-peak on 10 cardiac cycles; arterial waveform width for each cardiac cycle was set to 1.4 times of R-R interval for the respective cycle
5) SPH, BPP and PPG foot, peak, tidal, dicrotic notch peak and foot fiducial points were detected
6) The SI, RI, AI, AIx, EI, EEI and Dai indexes were calculated, see the supplementary document for calculation of indexes.
7) Thr agreement analysis was performed via Bland-Altman analysis and verified by weighted Kappa for BPP and PPG waveform indexes against SPH waveform indexes, individually.

TABLE 2. The bland-altman and kappa analysis, SPH against BPP on left and SPH against PPG on right.

	BPP Indexes Vs SPH Indexes								PPG Indexes Vs SPH Indexes							
	Kappa	Systematic Difference			Limit of Agreement				Kappa	Systematic Difference			Limit of Agreement			
Ind		LoA	Mean	SD	Lower limit	95% CI	Upper limit	95% CI		LoA	Mean	SD	Lower limit	95% CI	Upper limit	95% CI
RI	0.1407	0.0111	0.0032	0.0028	-0.0023	-0.0052 to 0.0005	0.0087	0.0059 to 0.0116	-0.0496	0.0247	0.0063	-0.0001	-0.0124	-0.0188 to -0.0060	0.0123	0.0059 to 0.0187
AIx	0.2425	0.0203	0.0063	0.0052	-0.0038	-0.0091 to 0.0014	0.0164	0.0112 to 0.0216	0.2543	0.0374	0.0095	0.0061	-0.0126	-0.0222 to -0.0029	0.0247	0.0151 to 0.0343
SI	0.3950	0.0923	-0.0356	0.0236	-0.0817	-0.1056 to -0.0579	0.0106	-0.0133 to 0.0344	-0.0445	0.4082	0.1041	-0.0413	-0.2453	-0.3507 to -0.1400	0.1628	0.0575 to 0.2682
AI	0.5596	0.1089	-0.0074	0.0278	-0.0619	-0.0899 to -0.0338	0.0470	0.0189 to 0.0751	0.2394	0.1906	-0.0486	-0.0264	-0.1217	-0.1709 to -0.0725	0.0689	0.0197 to 0.1181
Dai	0.2705	0.2415	-0.0635	0.0616	-0.1842	-0.2465 to -0.1219	0.0573	-0.0050 to 0.1196	0.0539	0.4389	0.1120	-0.0111	-0.2306	-0.3438 to -0.1173	0.2083	0.0951 to 0.3216
EI	0.2425	2.1303	-0.1618	0.5435	-1.227	-1.7766 to -0.6773	0.9034	0.3537 to 1.4530	0.2394	2.5695	0.6555	-0.0609	-1.3457	-2.0087 to -0.6828	1.2238	0.5608 to 1.8867
EEI	0.2425	2.1539	0.1631	0.5495	-0.9138	-1.4695 to -0.3581	1.2401	0.6843 to 1.7958	0.2394	2.6108	0.6660	0.0544	-1.251	-1.9246 to -0.5774	1.3598	0.6862 to 2.0334

TABLE 3. The regression and spearman's analysis for the arterial indexes, SPH against BPP waveform (on left) and SPH against PPG waveform (on right).

Indexes	Spearman's Rank Correlation		Linear Regression		Spearman's Rank Correlation		Linear Regression
SPH vs	Significance level	rho	r^2	Indexes	Significance level	rho	r^2
AI BPP	P=0.005	0.720	0.95	AI PPG	P=0.1440	0.429	0.22
SI BPP	P<0.0001	0.875	0.92	SI PPG	P=0.058	0.537	0.61
AIx BPP	P<0.0001	0.907	0.83	AIx PPG	P=0.034	0.588	0.66
EI BPP	P<0.0001	0.860	0.81	EI PPG	P=0.159	0.434	0.35
EEI BPP	P<0.0001	0.825	0.80	EEI PPG	P=0.0245	0.364	0.34
Dai BPP	P=0.003	0.747	0.77	Dai PPG	P=0.5533	0.181	0.09
RI BPP	P=0.194	0.385	0.50	RI PPG	P=0.7890	-0.0824	0.19

*Ascending order based on 'r^2' values of linear regression among the Indexes

8) The regression analysis and Spearman's rank correlation were performed for BPP and PPG waveform indexes against SPH waveform indexes, individually.

VII. RESULTS

The agreement analysis was performed via Bland-Altman analysis between, 1) PPG waveform arterial indexes to SPH waveform arterial indexes, and 2) BPP waveform arterial indexes against SPH waveform arterial indexes, individually, shown in figure 10, arranged in ascending order with respect to limit of agreement (LoA). The indexes calculated from the BPP waveforms has shown a narrower/closer limit of agreement (LoA) than indexes calculated from PPG waveform when compared against SPH waveform, individually. The indexes comparison based on LoA signifies the higher accuracy of BPP waveform than PPG waveforms. Where RI and AIx had the closest/narrowest LoA and EEI shown widest/highest LoA. To validate the trend shown by Bland-Altman, the weighted Kappa analysis (WKA) was used, where (none<0.2>slight<0.4>fair<0.6>moderate<0.8>perfect<1).

In WKA, among indexes of SPH waveform versus BPP waveforms, AI and SI indexes (on top of ascending order) showed the moderate relationship while the rest of the indexes showed fair relationship except RI which showed the slight relationship. The WKA among indexes of SPH waveform versus PPG waveforms, AIx, AI, EI and EEI indexes showed fair relationship and the rest of the indexes showed no relationship, shown in Table 2.

The outlier from each data set was removed and then regression analysis was performed to find the correlation of indexes of the BPP waveform and PPG waveforms against SPH waveform, individually, plots are shown in figure 11. The similar behavior as Bland-Altman analysis was observed, that BPP waveform indexes showed a higher correlation to SPH waveform than PPG waveform indexes correlation to SPH waveform. When regression values are arranged in ascending order AI, SI, AIx, EI, EEI and Dai of BPP waveform showed highest correlation. The Spearman's rank correlation was used to validate the trend shown by the regression analysis. The Spearman's rank correlation between indexes of the BPP waveform and SPH waveform showed that AIx, SI, EI (on top of ascending order) and EEI showed a very strong positive correlation, AI and Dai showed a strong correlation, and RI showed moderate correlation. In the Spearman's correlation between indexes of PPG waveform and SPH

waveform, SI showed the strong positive correlation while AIx, EI, EEI and AI showed moderate positive correlation and the rest of the indexes showed very weak correlation as shown in Table 3. Further details of these analyses are available in the supplementary document.

The 2 & 4-element WK models was estimated only for BPP waveform to SPH waveform for the radial artery branching from the wrist to distal phalanx in the index finger by using the MATLAB system identification toolbox. The accuracies of the individual transfer function of 2-element WK model was higher than 85% and the accuracies of the individual transfer function of 4-element WK model was higher than 98%. The parametric mean and standard deviation of transfer function are shown in supplementary notes.

VIII. DISSCUSION

With reference to SPH waveform, accumulatively the BPP AIx index performed best among all parameters. The overall best performances are shown by AI, EEI and SI indexes of BPP waveform which were supported by Wowern et. al. parametric results [5]. However, in our study, the BPP outperforms PPG at indexes on a one-to-one basis as well as in the overall performance. The Dai index showed a weak but significant relationship, whereas RI showed almost no significance among the BPP measured parameters.

The APG demarcation of the fiducial wave is mathematically complex and intensive, which becomes more difficult in PPG waveform, as the tidal wave is not easily visible. Whereas, in the BPP waveform the tidal wave was visible in all the subjects. This inconsistency has also been reported elsewhere [19]. The dicrotic notch and the tidal wave are consistently visible in BPP waveform, as found in this study, which makes the BPP waveform superior to the PPG waveform.

The clinical associations with cardiovascular diseases are well established in the literature for AIx and AI indexes [5], [9] to their relationship. It was out of scope for this study to reverify or establish any such relationship among the healthy and patients' groups.

Due to the high sensitivity of PVDF sensor to mechanical vibration, the BPP waveform sensing may be limited to stable posture to avoid motion artefacts. Likewise, it becomes a future topic to find the method which reveals the signal information underline the motion artefacts.

The 2-element WK model is a simpler function and can have an easier physiological interpretation for person-specific parameters; which will provide the possibility of adaptive tracking (suggested future work) as suggested by Mukkamala *et al.* [1].

The BPP is independent of the subject's skin color and the effect of cosmetics on skin's surface compared to PPG waveform. Another advantage is being operatorless makes more attractive compared to SPH waveform.

IX. CONCLUSION

The BPP measurement technique has shown to be unaided/operatorless, cheaper and easier to use compared to conventional tonometric devices and outperforms the conventional state-of-the-art PPG technique. In wearable technologies, assessment of arterial indexes may help the early detection and prevention of CVD.

APPENDIX

Supplementary notes (*).

ACKNOWLEDGMENT

The authors would like thank Professor Tara Moore for her help and support in this project.

REFERENCES

[1] R. Mukkamala, J.-O. Hahn, O. T. Inan, L. K. Mestha, C.-S. Kim, H. Töreyin, and S. Kyal, "Toward ubiquitous blood pressure monitoring via pulse transit time: Theory and practice," *IEEE Trans. Biomed. Eng.*, vol. 62, no. 8, pp. 1879–1901, Aug. 2015.

[2] M. Butlin, F. Shirbani, E. Barin, I. Tan, B. Spronck, and A. Avolio, "Cuffless estimation of blood pressure: Importance of variability in blood pressure dependence of arterial stiffness across individuals and measurement sites," *IEEE Trans. Biomed. Eng.*, vol. 65, no. 11, pp. 2377–2383, Nov. 2018.

[3] S. Elhani, T. J. Cleophas, and R. Atiqi, "Lifestyle interventions in the management of hypertension: A survey based on the opinion of 105 practitioners," *Netherlands Heart J.*, vol. 17, no. 1, pp. 9–12, Jan. 2009.

[4] L. Peter, N. Noury, and M. Cerny, "A review of methods for non-invasive and continuous blood pressure monitoring: Pulse transit time method is promising?" *IRBM*, vol. 35, no. 5, pp. 271–282, Oct. 2014.

[5] E. von Wowern, G. Östling, P. M. Nilsson, and P. Olofsson, "Digital photoplethysmography for assessment of arterial stiffness: Repeatability and comparison with applanation tonometry," *PLoS ONE*, vol. 10, no. 8, Aug. 2015, Art. no. e0135659.

[6] O. T. Inan, P.-F. Migeotte, K.-S. Park, M. Etemadi, K. Tavakolian, R. Casanella, J. Zanetti, J. Tank, I. Funtova, G. K. Prisk, and M. Di Rienzo, "Ballistocardiography and seismocardiography: A review of recent advances," *IEEE J. Biomed. Health Inform.*, vol. 19, no. 4, pp. 1414–1427, Jul. 2015.

[7] D. D. He, E. S. Winokur, and C. G. Sodini, "An ear-worn continuous ballistocardiogram (BCG) sensor for cardiovascular monitoring," in *Proc. Annu. Int. Conf. IEEE Eng. Med. Biol. Soc.*, Aug./Sep. 2012, pp. 5030–5033.

[8] A. B. Hertzman, "The blood supply of various skin areas as estimated by the photoelectric plethysmograph," *Amer. J. Physiol.-Legacy Content*, vol. 124, no. 2, pp. 328–340, Oct. 1938.

[9] M. F. O'Rourke, A. Pauca, and X.-J. Jiang, "Pulse wave analysis," *J. Hypertens.*, vol. 51, no. 6, pp. 507–522, Jun. 2001.

[10] W. W. Nichols and D. A. MacDonald, *McDonald's Blood Flow in Arteries: Theoretical, Experimental and Clinical Principles*. London, U.K.: Hodder Arnold, 2011.

[11] G. Janjua, J. Mclaughlin, D. Finlay, and D. Guldenring, "Wireless chest wearable vital sign monitoring platform for hypertension," in *Proc. 39th Annu. Int. Conf. IEEE Eng. Med. Biol. Soc.*, Jul. 2017, pp. 821–824.

[12] D. J. Korteweg, "Over voortplantings-snelheid van golven in elastische buizen," Ph.D. dissertation, Dept. Math. Phys., Univ. Amsterdam, Amsterdam, The Netherlands, 1878.

[13] J. Liu, B. P.-Y. Yan, W.-X. Dai, X.-R. Ding, Y.-T. Zhang, and N. Zhao, "Multi-wavelength photoplethysmography method for skin arterial pulse extraction," *Biomed. Opt. Express*, vol. 7, no. 10, pp. 4313–4326, Oct. 2016.

[14] W. Nitsche, "The use of piezofilms for noninvasive measurements of blood pressure," in *Blood Pressure Measurements*. Heidelberg, Germany: Steinkopff, 1990, pp. 27–33.

[15] M. Elgendi, "On the analysis of fingertip photoplethysmogram signals," *Current Cardiol. Rev.*, vol. 8, no. 1, pp. 14–25, Feb. 2012.

[16] J. Pan and W. J. Tompkins, "A real-time QRS detection algorithm," *IEEE Trans. Biomed. Eng.*, vol. BME-32, no. 3, pp. 230–236, Mar. 1985.

[17] M. F. O'Rourke, "Wave travel and reflection in the arterial system," *J. Hypertens. Suppl.*, vol. 17, no. 5, p. S45-7, Dec. 1999.

[18] M. Gao, W. C. Rose, B. Fetics, D. A. Kass, C.-H. Chen, and R. Mukkamala, "A simple adaptive transfer function for deriving the central blood pressure waveform from a radial blood pressure waveform," *Sci. Rep.*, vol. 6, no. 1, Dec. 2016, Art. no. 33230.

[19] S. C. Millasseau, J. M. Ritter, K. Takazawa, and P. J. Chowienczyk, "Contour analysis of the photoplethysmographic pulse measured at the finger," *J. Hypertension*, vol. 24, no. 8, pp. 1449–1456, Aug. 2006.

GHALIB MUHAMMAD WAQAS JANJUA received the bachelor's degree in electrical engineering from UET, Pakistan, in 2008, and the master's degree in digital system design and signal processing from NUST, Pakistan, in 2014. He is currently pursuing the Ph.D. degree with CHESS, as a Marie Curie Fellow, a training consortium funded by the European Union's Horizon 2020 Research and Innovation Programme. He was an Embedded Engineer with Horizon Tech Services Ltd., for 6.4 years, where he was promoted to Senior Embedded Engineer. He joined the Tyndall National Institute, Ireland, as an Engineer, working on the National Access Program, for 1.5 years, where he worked on wireless health monitoring systems, the IoT-based noncontactless temperature measurement devices, and smart dressing projects. He is an Early Stage Researcher involved in the development of noninvasive continuous cuff-less blood pressure monitoring systems. He is a solution-oriented professional with a proven track record in the IoT embedded system product development and signal processing, both within the industry and academic sectors. He has an excellent acumen-ship to research and development processes and procedures for product development. He is currently with the Nanotechnology and Integrated Bioengineering Centre, Ulster University, U.K.

DEWAR FINLAY is the Engineering Research Director of the Ulster University, where he is also a Professor of electronic systems. He is an Electronic Engineer and holds a Ph.D. degree in computing and a Postgraduate Certificate in Higher Educational Practice. His research focuses on healthcare technology with a specific emphasis on biosignal processing and analysis. He has published more than 100 articles (h-index 21) and supervised more than ten Ph.D. students to completion. He has attracted over £10 million in research funding, all related to the development of healthcare technology, and currently serves as a PI and CI on a number of EU H2020 projects in the area of connected health (CHESS, PATHway, and IC-Health). He has served as the Director of the University's M.Sc. in Health Informatics and is currently a member of the Board of Directors of Computing in Cardiology, Inc.

DANIEL GULDENRING received the Dipl.-Ing. (FH) degree in electrical engineering and the M.Eng. degree in mechatronics engineering from the Augsburg University of Applied Sciences, Augsburg, Germany, in 2009, and the Ph.D. degree from the School of Computing and Mathematics, Ulster University, Belfast, in 2013.

He is currently with the HTW Berlin, Berlin, Germany. His main areas of teaching are in electrical engineering and embedded systems. His main research is on medical devices, with a particular interest in biomedical signal processing for computerized electrocardiology.

Prof. Gueldenring is a member of the International Society for Computerized Electrocardiology. He has been serving on the Program Committee for Computing in Cardiology, since 2009.

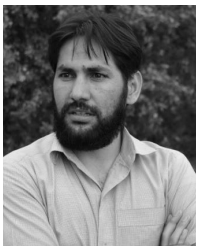

ATTA UL HAQ received the bachelor's degree in metallurgy and materials engineering from the Ghulam Ishaq Khan Institute of Engineering Sciences and Technology (GIKI), Pakistan, the master's degree in materials engineering from the Korea Advanced Institute of Science and Technology (KAIST), South Korea, and the Ph.D. degree in engineering from Ulster University, in 2017, as a prestigious Marie Curie Fellow, where he is currently a Postdoctoral Research Fellow with the Nanotechnology and Integrated Bioengineering Centre (NIBEC). His Ph.D. research is involved in nanoengineering of group IV nanocrystals by atmospheric pressure microplasmas.

JAMES MCLAUGHLIN graduated from NUU and later received the Ph.D. degree in physics from Ulster University. He is currently a Professor with the School of Engineering. He is also the Director of the Engineering Research Institute, the Director of the NIBEC, and a Physicist. He has been developing significant initiatives within research, technology-transfer, outreach, and teaching, since 1986. He has successfully cofounded a set of spin-out companies, including the highly successful connected health company, Intelesens-Ltd., and more recently, SiSaF-Ltd. He was a Consultant associated with key processes and patents with Heartscape and Heartsine. He has been honored as an Invited Speaker at over 30 international conferences. He has personally granted over £100m of funding, including NIBEC/BEST/SEAGATE-Consortium/NICAM/NANOTECTNI/NIACE/CACR/CHIC, and a new Healthcare Technology City Deal. He holds over 30 patents, including one for the world's bestselling disposable medical electrode. His salient disciplines address connected health, nanotechnology, and related biosensing/point-of-care diagnostic applications. He is a Fellow of the Institute of Physics and the Irish Academy of Engineering. He received a Senior-Distinguished Research Fellowship from Ulster. He also received an OBE for his services to research and economic development in U.K. He has attained excess of 300 publications (h-index 34) and supervised over 25 Ph.D. students. In recent years, his over-arching strategy is to develop a strongly connected health platform within the EU (as the Co-Director of the European Connected Health Alliance). This work involves linking bioengineering and computing sciences with sensor technology developed within NIBEC and thus, facilitating clinically led research initiatives to benefit the healthcare sector. He held positions on committees, such as RAE-2008 Materials Assessment Panel, a Matrix Panel Member and a Sub-Chair, EPSRC-College, NanoIreland Task Force/Chaired the Nanomaterials Panel, H2020-COST Action ENJECT, H2020 E-Health Strategy Board, Advisory Committee to KTN-Health Technologies, CCAN, MSSI, and the Cambridge Nano-DTC. He was the Chair and the Co-Founder of the European Connected Health Alliance and the Co-Chair of the Matrix NI Life and Health Sciences Strategy Panel. He also leads one of the last final seven teams in the £10m Qualcomm Tricorder Xprize Competition. He has recently co-led a £5m to Connected Health Innovation Centre (CHIC) and followed this with a new £7m Biodevices Laboratory.